



## Diversity and co-occurrence networks of bacterial and fungal communities on two typical debris-covered glaciers, southeastern Tibetan Plateau

Yang Hu <sup>a,b</sup>, Heather Fair <sup>c</sup>, Qiao Liu <sup>a</sup>, Ziwei Wang <sup>a, b</sup>, Baoli Duan <sup>a,\*</sup>, Xuyang Lu <sup>a,\*</sup>

<sup>a</sup> Key Laboratory of Mountain Surface Processes and Ecological Regulation, Institute of Mountain Hazards and Environment, Chinese Academy of Sciences, Chengdu, Sichuan 610299, China

<sup>b</sup> University of Chinese Academy of Sciences, Beijing 100101, China

<sup>c</sup> Department of Plant and Microbial Biology, University of Minnesota, Saint Paul, Minnesota 55108, USA

### ARTICLE INFO

**Keywords:**

Debris-covered glaciers  
Microbial community  
Microbial diversity  
High-throughput sequencing

### ABSTRACT

Debris-covered glaciers (DCGs) are globally distributed and thought to contain greater microbial diversity than clean surface continental glaciers, but the ecological characteristics of microbial communities on the surface of DCGs have remained underexplored. Here, we investigated bacterial and fungal diversity and co-occurrence networks on the supraglacial debris habitat of two DCGs (Hailuogou and Dagongba Glaciers) in the south-eastern Tibetan Plateau. We found that the supraglacial debris harbored abundant microbes with Proteobacteria occupying more than half (51.5%) of the total bacteria operational taxonomic units. The composition, diversity, and co-occurrence networks of both bacterial and fungal communities in the debris were significantly different between Hailuogou Glacier and Dagongba Glacier even though the glaciers are geographically adjacent within the same mountain range. Bacteria were more diverse in the debris of the Dagongba Glacier, where a lower surface velocity and thicker debris layer allowed the supraglacial debris to continuously weather and accumulate nutrients. Fungi were more diverse in the debris of the Hailuogou Glacier, which experiences a wetter monsoonal climate, is richer in calcium, has greater debris instability, and greater ice velocity than the Dagongba Glacier. These factors may provide ideal conditions for the dispersal and propagation of fungi spores on the Hailuogou Glacier. In addition, we found an obvious gradient of bacterial diversity along the supraglacial debris transect on the Hailuogou Glacier. Bacterial diversity was lower where debris cover was thin and scattered and became more diverse near the glacial terminus in thick, slow-moving debris. No such increasing bacterial pattern was detected on the Dagongba Glacier, which implies a positive relationship of debris age, thickness, and weathering on bacterial diversity. Additionally, a highly connected bacterial co-occurrence network with low modularity was found in the debris of the Hailuogou Glacier. In contrast, debris from the Dagongba Glacier exhibited less connected but more modularized co-occurrence networks of both bacterial and fungal communities. These findings indicate that less disturbed supraglacial debris conditions are crucial for microbes to form stable communities on DCGs.

### 1. Introduction

Glaciers and ice sheets cover approximately 10% of the earth's surface with forty-four percent of glaciers larger than 2 km<sup>2</sup> having debris present on the glacier surface (Herreid and Pellicciotti, 2020). More common in high mountain regions such as the Andes and the Himalayas, debris-covered glaciers (DCGs) have ablation zones covered by a nearly continuous layer of rock materials. Debris originates from periglacial slope deformations, rockfalls, avalanches, and landslides, as well as from the melt-out of englacial debris and atmospheric deposition of fine

materials. The size of debris ranges from fractions of a millimeter in diameter to greater than a meter and the thickness of debris on the ice surface ranges from millimeters to well over a meter (Compagno et al., 2022; Scherler et al., 2018). Due to the pronounced impacts of climate change on mountain ecosystems, mountain glaciers are experiencing dramatic size and volume reductions as global temperatures increase, and DCGs are predicted to become more widespread and prominent in the future (Westoby et al., 2020; Winter-Billington et al., 2022). DCGs are thought to contain greater microbial diversity than clean surface continental glaciers (i.e., Antarctica and Greenland), due to the

\* Corresponding authors.

E-mail addresses: [duanbl@imde.ac.cn](mailto:duanbl@imde.ac.cn) (B. Duan), [xylu@imde.ac.cn](mailto:xylu@imde.ac.cn) (X. Lu).

allochthonous material sourced from mountain slopes, which may accelerate microbial activity and soil development on the ice surface (Azzoni et al., 2015; Franzetti et al., 2013). Supraglacial debris as a study ecosystem is unique in that rather than an upslope migration of species with climate change, debris typically originates from higher altitude sources and migrates downward onto the ice due to weathering and erosion processes, with microbes being transported onto the ice surface. Therefore, supraglacial debris is not only a source of young soils at glacier foreheads as glaciers retreat, but is also an unexplored frontier to examine potential downward species migration from higher altitudes onto the glacier surface.

The composition, diversity, and biogeographical patterns of microbial communities have been well documented along glacier forefront chronosequences (Franzetti et al., 2020; Jiang et al., 2018; Zumsteg et al., 2012) and within supraglacial cryoconite holes on clean surface glaciers (Ambrosini et al., 2017; Smith et al., 2018) by using culture-dependent and culture-independent methods. Soil-dwelling communities of bacteria, fungi, archaea, nematodes, rotifers, and arthropods have been found to colonize the surfaces of DCGs (Azzoni et al., 2015; Franzetti et al., 2013). These microbial communities not only mediate the biogeochemical cycling of supraglacial ecosystems but also play a key role in driving soil development which allows for pioneering shrubs and trees to colonize limited surfaces of DCGs (Caccianiga et al., 2011; Fickert et al., 2022). Nevertheless, only a few studies have briefly described the composition and spatial structure of bacterial communities on DCGs (Franzetti et al., 2013; Sherpa et al., 2018). These studies reported that the dominant bacterial taxa of supraglacial debris were Actinobacteridae, Sphingobacteriales, and Burkholderiales, and the genus *Polaromonas*, which exhibit metabolic versatility and contribute to rock-weathering in cold environments. Furthermore, evidence from the Toklat Glacier (Alaska, USA) and Miage Glacier (Mont Blanc massif, Western Alps, Italy) demonstrated that chronosequences similar to those reported in glacier forefields exist on the surface of typical DCGs (Darcy et al., 2017; Franzetti et al., 2013; Gobbi et al., 2011). Specifically, bacterial, fungal, and arthropod communities have been shown to increase in complexity along the ablation zone, with microbial communities progressively transitioning from autotrophic to heterotrophic toward the glacier terminus (Franzetti et al., 2013). Their diversity and distribution patterns have been associated with environmental factors including ice ablation rate, pH, nitrogen availability, and organic carbon content (Darcy et al., 2017; Franzetti et al., 2013). Bacteria and fungi may be influenced by distinct environmental factors due to their difference in metabolic processes (Jiang et al., 2018), stress tolerance (de Vries et al., 2018; Shen et al., 2020), and substrate preferences (Sun et al., 2017). Exploring the bacterial and fungal assembly processes within debris with surrounding physicochemical properties is important in understanding the ecology of DCGs.

Microbes living together in a community interact frequently but their interrelationships are difficult to detect with standard bioinformatics analyses. Co-occurrence networks are a way to visualize the connections among microbial species and explore the co-existing species in a community based on significant (valid) and positive (robust) correlations (Barberán et al., 2012; Ma et al., 2017; Steinhäuser et al., 2008). Beyond microbial diversity, microbial co-occurrence patterns are significant in predicting the stability and resilience of an ecosystem (Barberán et al., 2012; de Menezes et al., 2017; Wagg et al., 2019). Moreover, the networks are used for identifying keystone taxa that influence ecosystem functioning (Banerjee et al., 2018; Dong et al., 2022). The microbial co-occurrence networks of glacial ecosystems have been used to explore the microbial assembly processes in glacier forefield soils (Dong et al., 2022; Jiang et al., 2019) and glacier-fed streams (Ren and Gao, 2019; Zhang et al., 2021). However, bacterial and fungal co-occurrence networks of supraglacial debris are not reported to the best of our knowledge.

The Dagongba (DGB) Glacier and Hailuogou (HLG) Glacier are two typical debris-covered temperate valley glaciers with lengths > 10 km at

Mt. Gongga, which is the representative area of monsoon temperate glaciers in western China. The glaciers in this region are retreating at greater rates than other places in Tibet and the glacier tongues contain some of the highest extents of supraglacial debris cover in the region (Li et al., 2010; Miles et al., 2020; Zhang et al., 2011; Zhang et al., 2016a). We chose the DGB Glacier and HLG Glacier because they are located at the same latitude and are geographically adjacent within the same mountain range, but have distinct climates, geology, and surface conditions (Liu et al., 2017; Liao et al., 2020a, 2020b; Fu et al., 2021). Our research objective was to characterize the microbial communities within supraglacial debris, which represents an under-explored extreme habitat. We examined the composition, diversity, and co-occurrence networks of both bacterial and fungal communities. In particular, we aimed to understand the potential relationships of physicochemical and environmental factors on the diversity of bacteria and fungi within these two unique glaciers. Our research questions were: 1) What is the composition and co-occurrence network of bacterial and fungal communities on supraglacial debris? 2) Are the bacterial and fungal communities different between these two debris-covered glaciers? If so, how do they differ? and 3) Which environmental factors best predict the bacterial and fungi diversity and geographic patterns of the debris-covered supraglacial ecosystem?

## 2. Materials and methods

### 2.1. Study Sites

Mt Gongga (7556 m a.s.l.) is the highest peak of the southeastern Tibetan plateau which serves as an important monsoonal climatic barrier and is the location of the most developed monsoonal temperate glaciers in China. In the past several decades the glaciers of the south-eastern Tibetan Plateau have been experiencing retreat at a faster rate than other glaciers of High Mountain Asia (Liu et al., 2017; Liao et al., 2020a, 2020b).

The Dagongba Glacier (21.2 km<sup>2</sup>) is on the west side of Mt. Gongga (29° 34'N, 101° 48'E) and the Hailuogou Glacier (25.7 km<sup>2</sup>) is on the east side of Mt. Gongga (29° 34'N, 101° 59'E) (Zhang et al., 2016a). The west side of Mt. Gongga is dominated by sunny weather and is influenced by the southwestern monsoon from the Indian Ocean with a mean annual air temperature of 2.2 °C and mean annual precipitation of 1151 mm (3700 m a.s.l. meteorological station). The climate of the east side of Mt. Gongga is dominated by cloudy weather and influenced by the south-eastern monsoon from the Pacific Ocean and has a mean annual air temperature of 3.9 °C and mean annual precipitation of 1938 mm (3000 m a.s.l. meteorological station) (Su et al., 1993; Su et al., 1996). The terrain of Mt. Gongga is steeper on the eastern slope and lower gradient on the western side with the dominant lithology being granite. DGB is debris-covered from approximately 4900 m a.s.l. to the glacier terminus at 3965 m a.s.l., with an average slope of 7.3°. HLG is debris-covered from 3700 m a.s.l. to the glacier terminus at 3015 m a.s.l., with an average slope of 16° (Fu et al., 2021; Zhang et al., 2011; Zhang et al., 2016a). Furthermore, DGB Glacier has greater mean debris thickness and lower mean surface velocity than the HLG Glacier, which has a warmer climate but a less stable surface condition (Table 1).

### 2.2. Supraglacial debris sampling

We collected debris samples using aseptic techniques from the surface of the supraglacial debris to a depth of 15 cm in July 2020. Sampling sites were distributed along the middle transect of the glacier tongues to avoid newly exposed debris from hillslope rock falls. The distance between each sampling site was between 150 and 500 m (Fig. 1, Table S1). Based on accessibility and sufficient distance between sites, seven sites were selected from 4018–4209 m a.s.l. on the DGB Glacier (D1 to D7) and 10 sites were selected from 2998 to 3567 m a.s.l. on the HLG Glacier (H1 to H10) (Fig. 1). At each site, wet debris samples were

**Table 1**

Characteristics of Dagongba (DGB) and Hailuogou (HLG) Glaciers.

	Dagongba Glacier	Hailuogou Glacier
Aspect	West side of Mt. Gongga	East side of Mt. Gongga
Elevation (m a. s. l.)	3965–6684	3015–7556
Mean annual precipitation(mm)	1151	1938
Area, Length	21.2 km <sup>2</sup> , 13.1 km	25.7 km <sup>2</sup> , 11 km
Mean slope (°)	7.3	16
Debris coverage (%)	22.9	22
Annual expansion of debris covered area (%)	3.2%	0.9%
Mean debris thickness (m)	1.12	0.72
Mean surface velocity (m.a <sup>-1</sup> )	4.67	43.53
Dominant stratum	Early Triassic, metamorphic rocks	Paleozoic, deep metamorphic rocks; Ancient magmatic rocks
Dominant lithology	granite	hornblende + biotite diorite with K-feldspar megacrystic granite
Dominant plant	dominated by shrubs from family of <i>Salix</i> , mainly <i>Salix rhododendrifolia</i>	colonized by herbs only on the terminus, mainly <i>Chamerion conspersum</i>

Precipitation was obtained from Su et al. (1993) and Su et al. (1996). Glacier area, length, and mean slope were obtained from Zhang et al. (2016a). Debris coverage (2019) and annual expansion rates of debris covered area (1990–2019) was obtained from Liao et al. (2020a). Debris thickness (DT) less than 50 cm was measured with a steel ruler in the field. Debris > 50 cm was calculated by empirical models and kinetic surface temperature maps (30 × 30 m<sup>2</sup>, Landsat-8/TIRS imagery, July 2020). Glacier surface velocity (GSV) was calculated by the temperature-index mass balance model (Liu and Liu, 2015a; Zhang et al., 2011; Zhang et al., 2019). Stratum and dominant lithology are obtained from Searle et al. (2016). Dominant plant were investigated in July of 2020.

collected from seven plots (1 × 1 m), homogenized into one composite sample, and sieved with a 2 mm mesh. All plant residues were removed and only debris material < 2 mm was collected for microbial sequencing, a total of 17 composite site samples comprised of 119

subsampled plots were collected. Those samples were placed on ice in the field and kept at 4 °C for a few hours during transport to the laboratory. In the laboratory, the debris samples were divided into three parts: one 50 g subsample from each site was placed in a sterile freeze-storage tube, and stored at 80 °C for molecular analysis. 100 g of debris from each site was stored in a sealed bag and maintained at 4 °C for physicochemical analyses. 200 g from each site was air-dried and stored in a sealed bag for further physicochemical analyses.

### 2.3. Physicochemical analysis of debris

Physicochemical characteristics of the debris were determined according to standardized soil techniques (Bao, 2000). Particle composition (%) (clay, silt, and sand) was measured using the pipette method. We mixed a soil: water (1:2.5) slurry to measure pH with a digital pH meter (FE20, Mettler-Toledo Instruments, China). Total nitrogen (TN), total carbon (TC), and organic matter (OM) were measured using an element analyzer (Vario TOC cube; Elementar, Langenselbold, Germany). Ammonium-N (NH<sub>4</sub>-N) and nitrate-N (NO<sub>3</sub>-N) were measured using the colorimetric method with a UV-vis spectrophotometer (UV-1800, Shimadzu, Japan; cuvette of Brand, Germany). Alkali-hydrolyzable nitrogen (AN) content was measured by alkaline hydrolysis diffusion method, while available phosphorus (AP) content was measured by Mo-Sb anti-spectrophotometer method, and available potassium (AK) content was measured by atomic absorption spectro-photometry. Metals Al - aluminum, Fe - iron, Ca - calcium, K - potassium, Mg - magnesium, Na - sodium, P - phosphorus, and Mn - manganese) were measured by an inductively coupled plasma optical emission spectrometer (ICP-OES, Optimal 2000 DV; Perkin-Elmer, USA).

### 2.4. DNA extraction and processing

DNA was extracted from 0.5 g of debris using the DNeasy® PowerSoil® Kit (Cat. No. 12888, QIAGEN GmbH, Hilden, Germany). The purity and quantity of DNA for each sample were verified using a NanoDrop 2000 instrument and agarose gel electrophoresis. The diluted genomic DNA (1 ng/mL) was used as a template for polymerase chain reaction (PCR) amplification with the barcoded primers and Tks Gflex DNA Polymerase (Cat. No. R060B, Takara Biochemicals, Beijing, China).

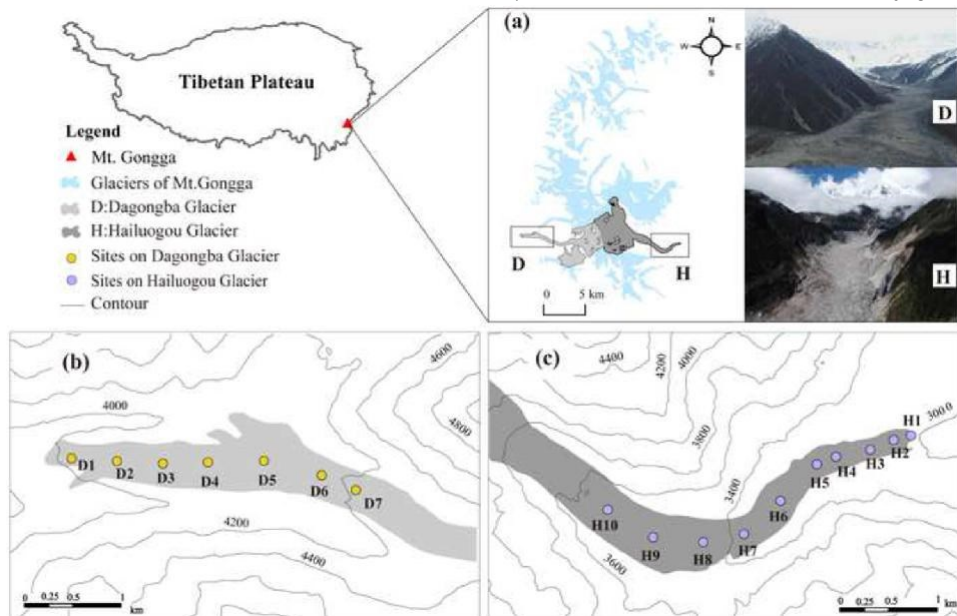


**Fig. 1.** Location of the Dadongba (D) and Hailuogou (H) Glacier study sites on the Tibetan Plateau (a) and microbial sampling sites (b & c). Samples were collected from sites at the Dadongba Glacier (D1-D7) (b) and Hailuogou Glacier (H1-H10) (c) in July 2020, Ganze Tibetan Autonomous Region, Sichuan, China.

The V3-V4 variable regions of the 16 S rRNA gene were amplified with universal primers 343 F and 798 R (Nossa et al., 2010; Wu et al., 2016), and the ITS 1 variable regions were amplified with universal primers ITS1F and ITS2 R (Mukherjee et al., 2014; Schoch et al., 2012). The primer sequences are provided in Table S2. The first round of PCR amplification was performed with 1  $\mu$ l (50 ng) of template DNA in 30  $\mu$ l reactions, employing an initial denaturation of 94 °C for five minutes, followed by 26 cycles (30 s at 94 °C, 30 s at 56 °C and 20 s at 72 °C), and a final extension for 5 min at 72 °C. Amplicon quality was visualized using gel electrophoresis, purified with AMPure XP beads (Beckman Coulter, Brea, CA, United States), and 1  $\mu$ l pf the products from the first round was used as a template in 30  $\mu$ l reactions for the second round of PCR (seven cycles). After being purified with the AMPure XP beads, the final amplicon was quantified using the Qubit dsDNA Assay kit (Cat. No. Q32854, Life Technologies, Grand Island, NY, United States). Equal amounts of purified amplicon were pooled for subsequent sequencing (Nossa et al., 2010; Wu et al., 2015). High-throughput sequencing of amplicons was performed on the Illumina MiSeq platform (Illumina, San Diego, CA, United States) at OEbiotech company (Shanghai, China). Sequencing data for bacterial and fungal communities were deposited in the National Center for Biotechnology Information (NCBI) Sequence Read Archive (<http://trace.ncbi.nlm.nih.gov/Traces/sra/>) under the accession numbers PRJNA797905 (bacteria) and PRJNA798561 (fungi).

Raw sequencing data were stored in the FASTQ format. Paired-end reads were then joined using Trimmomatic software (Bolger et al., 2014) and trimmed and assembled using FLASH software (10 bp, 200 bp, 20%) (Reyon et al., 2012). QIIME software was used to denoise and remove chimeras (Caporaso et al., 2010). Bacterial and fungal taxonomic assignments were conducted using the RDP classifier (Wang et al., 2007) and BLAST (Altschul et al., 1990) and clustered into operational taxonomic units (OTUs) using a 97% identity threshold via VSEARCH software (Rognes et al., 2016). The valid tags, mean length, and OTU counts for bacteria and fungi are listed in Table S3.

## 2.5. Statistical analysis

R (version 4.1.2) was used to perform all statistical analyses (R Core Team, 2021; Wickham, 2016). We first assessed the data for normality using the Shapiro-Wilk test and homogeneity of variances with the Bartlett test. The Wilcoxon rank-sum exact test was used to evaluate the differences in environmental variables between DGB and HLG with the agricolae package (Mendiburu, 2010). Venn diagrams were used to show common and endemic OTUs among sites with the ggVennDiagram package (Gao et al., 2021). The Bray-Curtis dissimilarity of bacterial and fungal communities was visualized by non-metric multidimensional scaling (NMDS) by using the metaMDS function in the package vegan (Dixon, 2003), with acceptable stress < 0.2. Analysis of similarities (ANOSIM) (Somerfield et al., 2021) was performed by using the anosim function with the vegan package to test the significance in Bray-Curtis dissimilarity ranks of microbial communities between groups and within groups. Microbial alpha diversity was represented by the Chao1 and Shannon indexes. The Wilcoxon rank-sum exact test was used to evaluate the differences in the diversity and relative abundance of dominant microbes between the two glaciers. Spearman's correlation between Shannon diversity and environmental variables was performed by the cor function, and the significance matrix was tested by cor\_pmat function in the package ggcormplot (Wei and Simko, 2017). All the environmental variables used in the correlation analysis have been normalized by the decostand function in the vegan package. Pearson linear correlation was used to link the distance from the glacier terminus with microbial Shannon diversity.

## 2.6. Microbial co-occurrence network analysis

Co-occurrence networks were constructed based on all possible

Spearman's rank correlations among species to explore the relationships between different microbial species and predict keystone taxa in each microbial network. The nodes and edges represented species and correlations among species, respectively, which are the two components used to form the co-occurrence network. The matrix of the nodes and edges was calculated using the corAndPvalue function with the WGCNA package (Langfelder and Horvath, 2008) based on the top 100 most abundant OTUs, with the valid and robust ( $p < 0.01$ ,  $|R| > 0.6$ ) relationship (Barberan et al., 2012; Ma et al., 2017; Steinhauser et al., 2008). P values were corrected for multiple testing using the p.adjust function (method = 'BH') with the stats package (Benjamini and Hochberg, 1995). Then the co-occurrence networks were visualized with Gephi software (Bastian et al., 2009). The co-occurrence network topological properties including the clustering coefficient of nodes, properties of the edges (positive % vs negative %), average degree, graph density, and modularity were calculated by Gephi software and used to evaluate the complexity and stability of microbial networks (Zhao et al., 2016).

## 3. Results

### 3.1. Physiochemical characteristics of debris

The supraglacial debris characteristics of the DGB Glacier and HLG Glacier differed substantially (Wilcoxon rank sum test,  $p < 0.05$ , Fig. 2). Specifically, supraglacial debris on the DGB Glacier had a greater percentage of clay and silt, and a greater TC, TN, OM, NO<sub>3</sub>-N, AN, AP, and AK content in comparison with HLG (Fig. 2a). Moreover, supraglacial debris in the DGB Glacier has a higher content of metals including Al, Fe, K, Na, and Mn, but supraglacial debris in HLG was characterized by a significantly greater percentage of sand and higher content of Ca (Fig. 2b).

### 3.2. Composition of bacterial and fungal communities

Good's coverage value of both bacterial and fungal communities exceeded 0.97, indicating that both had a high depth of Illumina sequencing (Table 2). We obtained 1164,650 high-quality bacterial 16 S rRNA sequences and 1145,316 high-quality fungal ITS-1 sequences, with valid lengths of 416.91 ( $\pm 1.75$ ) bp in bacteria and 265.59 ( $\pm 11.78$ ) bp in fungi, respectively (Table S3). 18,965 bacteria OTUs and 4440 fungi OTUs were obtained after clustering at 97% similarity (Table S3). From the core of the Venn diagram, there were 314 bacteria OTUs present in all sites, but only two fungi OTUs were present in all sites (Fig. S1). There was no significant difference in the number of bacteria OTUs between DGB and HLG, but the number of fungi OTUs was greater in HLG than in DGB (Wilcoxon rank sum test,  $p < 0.05$ ) (Fig. S1).

The dominant bacteria phyla (relative abundance >1%) were Proteobacteria, followed by Bacteroidetes, Actinobacteria, Gemmatimonadetes, Acidobacteria, Firmicutes, and Nitrospirae, accounting for 96.6% of the total bacterial sequences. Within the top 96.6% of bacterial sequences greater than 50% were comprised of Proteobacteria (51.5%) (Fig. 3a, Table S4). The dominant fungi phyla (relative abundance >1%) were Ascomycota, followed by Basidiomycota, Zygomycota, and Chytridiomycota, accounting for 87.6% of total fungal sequences (Fig. 3b, Table S4). The dominant bacteria were evenly distributed across all sites, while dominant fungi were randomly distributed in only some of the sites, particularly when examined at the lower taxonomic levels (Fig. 3c & 3d, Fig. S2). In addition, the dominant bacteria families were *Burkholderiaceae* (Betaproteobacteria), *Chitinophagaceae* (Bacteroidetes), and *Sphingomonadaceae* (Alphaproteobacteria) (Fig. 3c). Dominant fungi families were *Thelephoraceae*, *Strophariaceae*, and *Sebacinaceae* (Agaricomycetes) (Fig. 3d).

Both bacterial (stress=0.034) and fungal (stress=0.091) communities were well separated by glaciers from the horizontal axis of the NMDS (Fig. 4a & b), ANOSIM further indicated that both the bacterial

(a) **Glacier** **Dagongba** **Hailuogou**

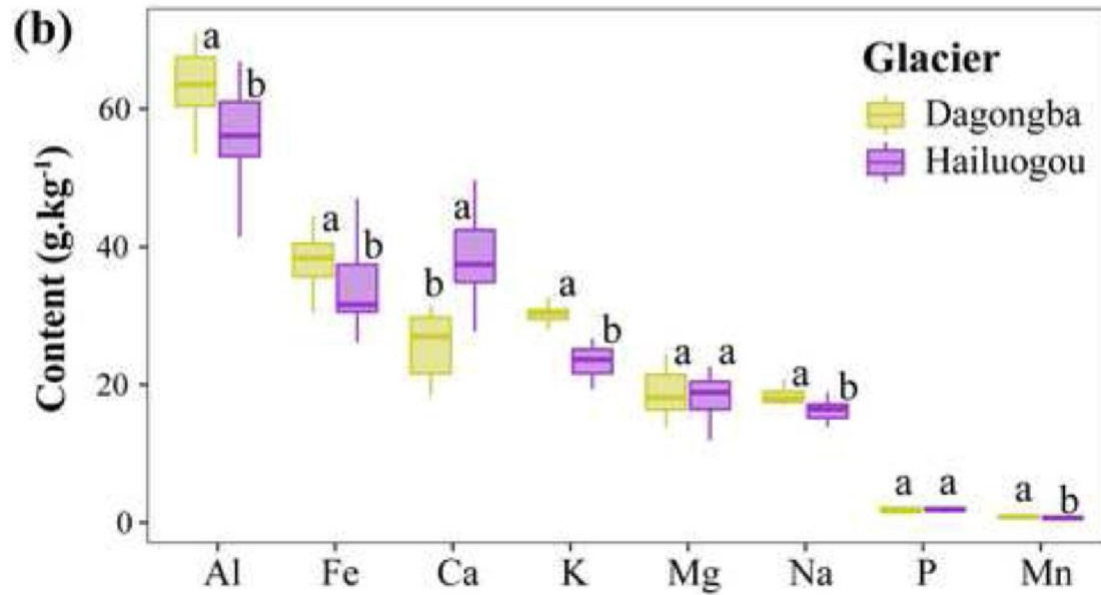
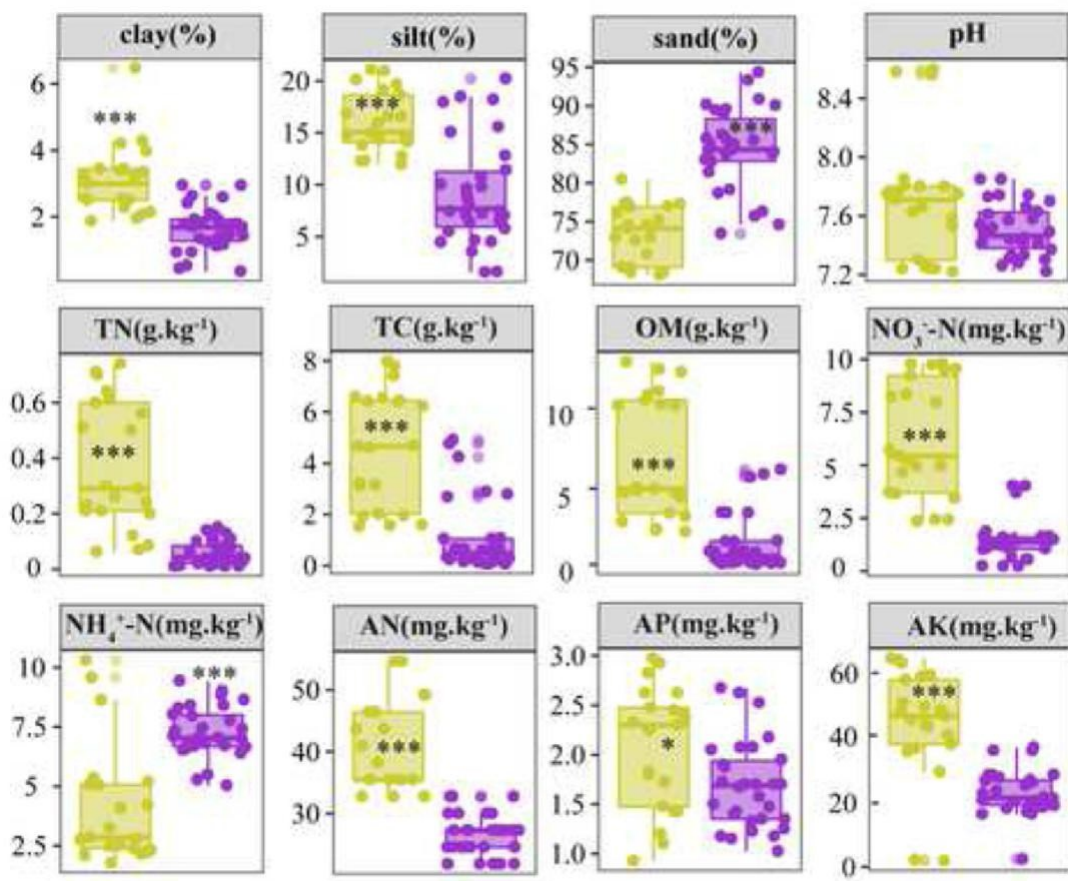


**Fig. 2.** Glaciological parameters and physicochemical characteristics of debris samples from Hailuogou and Dagongba Glaciers. Abbreviations are as follows: TN - total nitrogen, TC - total carbon, OM - organic matter, NH<sub>4</sub><sup>+</sup>-N - ammonium nitrogen, NO<sub>3</sub><sup>-</sup>-N - nitrate nitrogen, AN - Alkali-hydrolyzable nitrogen, AP - available phosphorus; AK - available potassium. Al: - aluminum, Fe - iron, Ca - calcium, K - potassium, Mg - magnesium, Na - sodium, P - phosphorus, and Mn - manganese. Error bars indicated the standard deviation, \*\*, \*\* and \*\*\* indicate significant differences at  $p < 0.05$ ,  $p < 0.01$ , and  $p < 0.001$  based on the Wilcoxon rank sum exact test, respectively. Different letters indicate significant ( $p < 0.05$ ) differences among glaciers based on the Wilcoxon rank sum exact test.

**Table 2**

Mean (SE) of alpha diversity within microbial communities in the supraglacial debris of the Dagongba (DGB) and Hailuogou (HLG) Glacier. Samples were obtained during July 2020, Mt. Gongga, Sichuan, China. Different letters indicate a significant difference (Wilcoxon rank sum test) among glaciers at  $p < 0.05$ .

Indices	Glaciers	
	DGB (n = 7)	HLG (n = 10)
Bacteria	Goods coverage	0.972 ( $\pm 0.003$ ) a
	Chao1	6242.51 ( $\pm 469.35$ ) a
	Shannon	10.27 ( $\pm 0.3$ ) a
Fungi	Goods coverage	0.9980 ( $\pm 0.000$ ) a
	Chao1	571.92 ( $\pm 107.18$ ) b
	Shannon	4.60 ( $\pm 1.31$ ) b

(ANOSIM:  $R=0.907$ ,  $p < 0.01$ ) and fungal (ANOSIM:  $R=0.864$ ,  $p < 0.01$ ) community composition was markedly different between the glaciers, with the bray-Curtis rank similarity between glaciers is greater than the similarity within the glaciers (Fig. 4c & d). Interestingly, bacterial communities clustered more tightly within the glaciers, while fungal communities were well separated within the glacier, indicating that fungi show greater variation across sites than bacteria (Fig. 4a & b).

### 3.3. Microbial diversity and environmental factors

Based on the chao1 and Shannon index, fungi were more diverse in

the debris of HLG than in DGB (Table 2, Fig. S3). Based on Spearman's correlation between Shannon diversity and environmental variables, we found that bacterial diversity significantly correlated with many of the debris physiochemical characteristics, including the percentage of clay, the content of TN, TC, OM, NO<sup>-3</sup>-N, the content of Fe, Ca, and P ( $p < 0.05$ ) (Table 3). Specifically, the percentage of clay, the content of TN, TC, OM, NO<sup>-3</sup>-N, and the content of metal Fe positively correlated with bacterial diversity, while the content of Ca and P negatively correlated with bacterial diversity. Fungal diversity negatively correlated with the percentage of clay in debris ( $R=0.731$ ,  $p < 0.01$ ), but positively correlated with the metal content of Ca, Mg, and P ( $p < 0.05$ ) (Table 3). Furthermore, the distance from the glacier terminus was negatively correlated with bacterial Shannon diversity in HLG ( $R=0.89$ ,  $p < 0.01$ ) (Fig. 5a). However, fungal diversity did not exhibit a distinct pattern along the supraglacial debris transect with distance from the glacier terminus having no significant effect on the fungi Shannon diversity of both the DGB Glacier and HLG Glacier (Fig. 5b).

### 3.4. Microbial co-occurrence patterns and hub species

The microbial co-occurrence network characteristics of supraglacial debris exhibited major differences between the glaciers. On the HLG Glacier, both bacterial and fungal co-occurrence networks had greater edges, average degree, and graph density than the DGB Glacier (Fig. 6, Table S5). On the DGB Glacier both bacterial and fungal co-occurrence networks had a higher value of modularity ( $>0.8$ ), indicating that

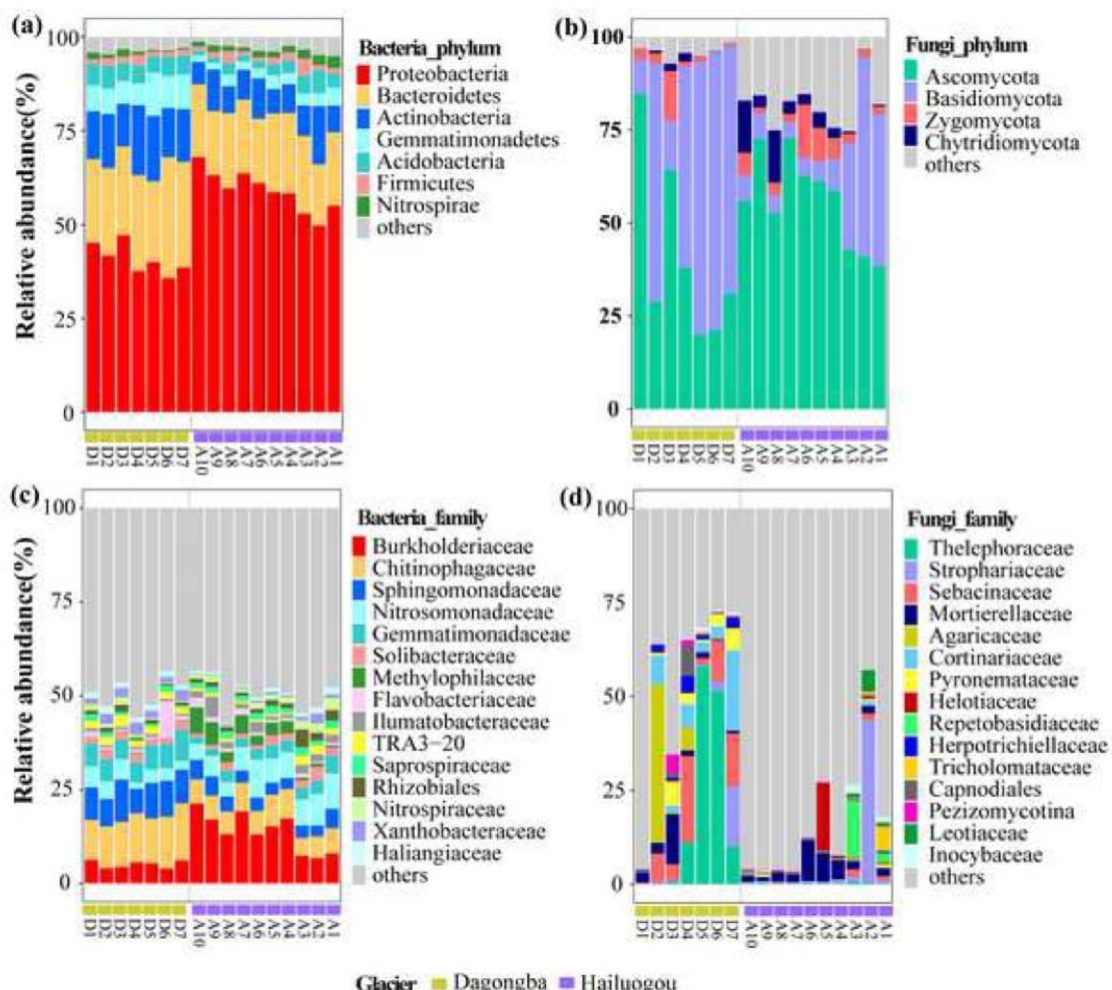


**Fig. 3.** Relative abundance of dominant phyla of bacteria and fungi (a & b) and families of bacteria and fungi (c & d) across glaciers and sites. Samples were collected from sites on the Dagongba Glacier (D1-D7) and Hailuogou Glacier (H1-H10) in July 2020, Ganze Tibetan Autonomous Region, Sichuan, China.

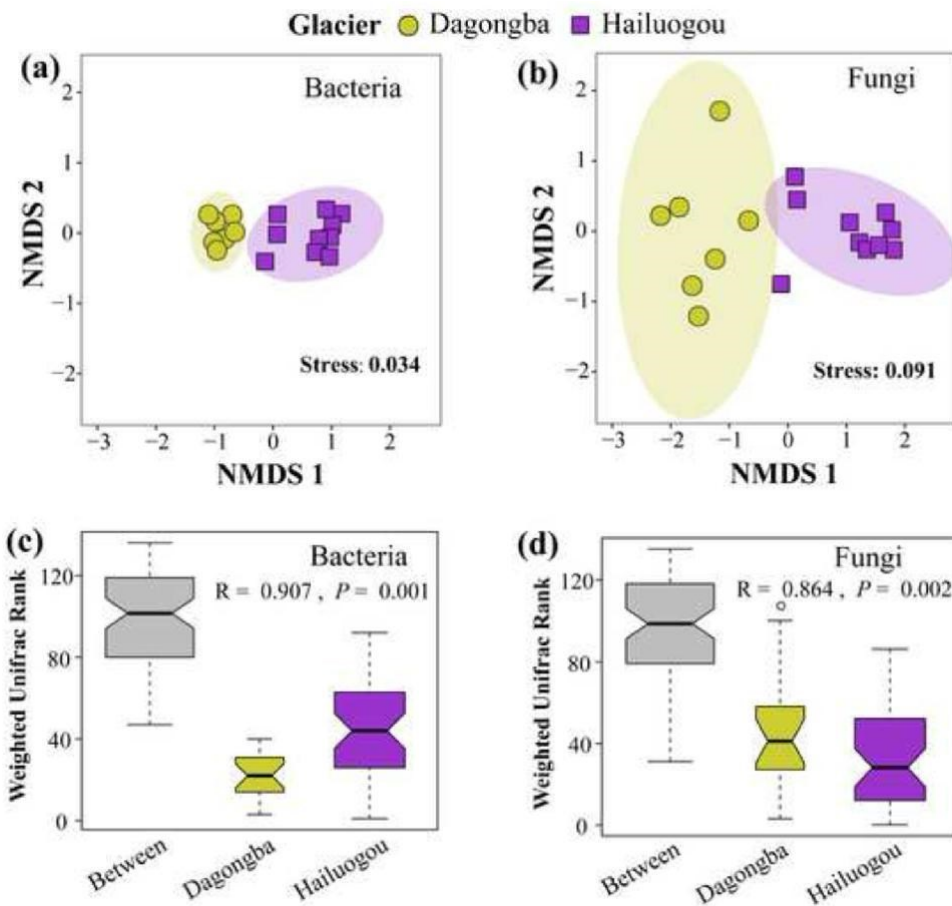


**Fig. 4.** Non-metric multidimensional scaling (NMDS) for bacterial (a & c) and fungal (b & d) communities. A stress value  $< 0.05$  indicate good fit,  $< 0.1$  are considered fair,  $> 0.2$  is deemed suspect. Ellipses represent 95% confidence intervals. Analysis of similarities (ANOSIM) plot showing Bray-Curtis dissimilarity ranks between glaciers and within glaciers at a significant level of  $p < 0.05$ .

bacterial and fungal co-occurrence were less connected but more modularized on the DGB Glacier than the HLG Glacier. Bacterial and fungal co-occurrence networks exhibited different patterns. In particular, the HLG Glacier bacterial co-occurrence networks were comprised of highly connected OTUs with low modularity. However, the fungal co-occurrence network of the HLG Glacier was less connected and divided into more modules. Moreover, bacterial co-occurrence networks had a slightly higher ratio of positive correlations on the DGB than HLG but the fungi co-occurrence networks showed high ratios of positive correlations in both the DGB and HLG glaciers.

The nodes (each node is represented by one OTU) with a greater average degree are highly linked with many other nodes (i.e., hubs), which play an important role in maintaining the structure of the co-occurrence networks. Most bacterial hubs belonged to the phyla Proteobacteria in co-occurrence networks (Fig. 6, Fig. S4). On the DGB Glacier bacterial co-occurrence networks hosted hubs comprised of *Segetibacter* (Bacteroidetes), whereas, on the HLG Glacier, the hubs were comprised of *Pseudorhodobacter* and *Polaromonas* (Proteobacteria). In fungal networks, fungi from the phyla Ascomycota represented most of the hubs, such as *Geopora* in DGB and *Pezoloma* in HLG. As well, *Mor-tierella* from Zygomycota was also listed as a hub (Fig. 6, Fig. S4).

#### 4. Discussion

##### 4.1. Influences of supraglacial debris on microbial diversity pattern

The phylum Proteobacteria occupied more than half (51.5%) of the bacterial taxa on the supraglacial debris of Dagongba (DGB) and

Hailuogou (HLG) glaciers. This pattern is in line with a previous study conducted by Darcy et al. (2017) in the supraglacial debris habitat of the Middle Fork Toklat Glacier (Alaska), as well as other glaciated environments from the Tibetan Plateau (Liu et al., 2015b; Liu et al., 2022). Moreover, Proteobacteria is a phylum reported commonly from glaci-ated environments around the globe (Sajjad et al., 2021; Sherpa et al., 2021), and is characterized by phylogenetic, morphological, physio-logical, and metabolic diversity (Kersters et al., 2006). *Burkholderiaceae*, *Chitinophagaceae*, and *Sphingomonadaceae* represented the predominant bacterial families of the DGB and HLG Glaciers. Likewise, *Burkholderiales* and *Sphingobacteriales* were reported as the dominant bacteria of supraglacial debris in the Italian Alps (Franzetti et al., 2013), and within other glacial environments such as cryoconite holes (Ambrosini et al., 2017). Before this study, the fungal communities of supraglacial debris had only been identified from the Toklat Glacier (Darcy et al., 2017). We found that on the DCGs from southeast Tibetan, the dominant fungi were the families *Thelephoraceae*, *Strophariaceae*, and *Sebacinaceae*, all of which are in the class Agaricomycetes within Basidiomycota. Most species from Basidiomycota, like those within Ascomycota, produce spores that allow dispersal via aerial migration which may be the reason they have been observed as dominant fungi in periglacial environments in different geographic locations (Franzetti et al., 2020; Jiang et al., 2018; Zumsteg et al., 2012). As well, fungi in the class Agaricomycetes have been observed to dominate in glaciated environments such as ice, snow (Perini et al., 2019a and 2019b), and recently deglaciated soils from glacial retreat areas (Fernandez-Martinez et al., 2017).

Despite the fact that the DGB and HLG Glaciers are geographically adjacent within the same mountain range, they have different climates,

**Table 3**

Spearman's correlation between microbial diversity and environmental variables of the debris-covered Dagongba and Hailuogou Glaciers, Sichuan, China. Abbreviations are as follows: 1) Nutrients: TN - total nitrogen, TC - total carbon, OM - organic matter, NH<sub>4</sub><sup>+</sup>-N - ammonium nitrogen, NO<sub>3</sub><sup>-</sup>-N - nitrate nitrogen, AN - Alkali-hydrolyzable nitrogen, AP - available phosphorus; AK - available potassium; 2) Elemental metals: Al - aluminium, Fe - iron, Ca - calcium, K - potassium, Mg - magnesium, Na - sodium, P - phosphorus, Mn - manganese. \*\*, \*\*\*, and \*\*\* indicate significant difference at " $p < 0.05$ ", " $p < 0.01$ ", and " $p < 0.001$ " based on the Spearman's correlation, respectively.

Variables	Bacteria	Fungi
clay	Shannon <b>0.581 **</b>	Shannon <b>-0.713 *</b>
silt	0.032	-0.326
sand	-0.48	0.172
pH	-0.596	0.017
TN	<b>0.613 *</b>	-0.588
TC	<b>0.667 *</b>	-0.502
OM	<b>0.654 *</b>	-0.505
NO <sub>3</sub> <sup>-</sup> -N	<b>0.593 *</b>	-0.645
NH <sub>4</sub> <sup>+</sup> -N	-0.404	0.203
AN	0.135	-0.451
AP	-0.01	-0.309
AK	0.395	-0.449
Al	0.289	-0.157
Fe	<b>0.424</b>	-0.346
Ca	<b>-0.404</b>	<b>0.444 *</b>
K	0.191	-0.461
Mg	-0.277	<b>0.451 *</b>
Na	-0.147	-0.206
P	<b>-0.691</b>	<b>0.426 *</b>
Mn	0.137	-0.005

geology, and surface conditions, which likely paved the way for the development of distinct microbial communities. Previous studies have reported that the development of microbial communities on supraglacial debris was limited by nitrogen and phosphorus content (Darcy and Schmidt, 2016; Schmidt et al., 2016). This study found that bacterial diversity was positively correlated with total nitrogen (TN), total carbon (TC), organic matter (OM), and ammonium nitrogen (NO<sub>3</sub><sup>-</sup>-N) which partially supports previous findings. Moreover, glaciers with greater ice flow velocities may be similar to a large-scale disturbance and serve as an important limiting factor for microbial community development on glacier surfaces (Caccianiga et al., 2011). In this study, glacier surface ice velocity was significantly ( $P < 0.05$ ) correlated with nutrients including total nitrogen (TN), total carbon (TC), ammonium nitrogen (NH<sub>4</sub><sup>+</sup>-N), Alkali-hydrolyzable nitrogen (AN), calcium (Ca), and potassium (K) (Table S6). The slower surface velocity of the DGB Glacier may have allowed the supraglacial debris to continuously weather and

accumulate nutrients. Notably, the supraglacial debris from HLG had significantly greater levels of calcium than the DGB Glacier, in line with reports by Liu et al. (2009) which found that the supraglacial debris from HLG was enriched in calcium oxide (CaO). Fungi were more diverse in supraglacial debris from HLG than in DGB, which is likely associated with the Ca content of the debris. Ca is known to be important in maintaining the stability of enzymes involved in fungal cell survival and the formation of fungal spores (Dzurenko et al., 2021; Liu et al., 2015b). Interestingly, in glacial retreat chronosequence research (Brown and Jumpponen, 2014) and environmental soil studies (Sun et al., 2017), the presence of plants has been found to have a stronger effect in shaping fungal diversity than in shaping bacterial diversity due to the symbiotic relationships between fungi and plants. The DGB Glacier, with a slower ice velocity and thicker debris cover than the HLG Glacier, is colonized by more pioneering plants on its surface. This suggests that the physicochemical differences between the debris and the presence of more plants and bushes on the DGB Glacier may be reducing the overall potential fungal diversity due to the greater dominance of specific fungal taxa that specialize in symbiotic relationships with plants.

There was an obvious gradient of bacterial richness along the supraglacial debris transect of HLG Glacier, with bacteria becoming more diverse near the glacial terminus. The gradient of bacteria diversity is possibly explained by the variations of debris stability and age which are controlled by glacier velocity and slope angle along the tongue of the HLG Glacier. Specifically, the HLG Glacier has a high ice velocity rate below the icefall at 3450–3600 m a.s.l. where the debris cover is thin and patchy, but the velocity slows as altitude decreases and the debris cover thickens (Zhang et al., 2011). From the field data of Zhang et al. (2016a), the mean thickness of supraglacial debris increases from 0.09 m at the upper tongue to 0.40 m at the glacial terminus. Obviously, debris near the glacier terminus had a longer and more stable exposure period which is more suitable for the colonization and development of bacterial communities originating from upslope regions. A similar pattern was reported on the Toklat Glacier in Alaska (Darcy et al., 2017) and Miage Glacier in Italy (Franzetti et al., 2013). These findings and ours suggest that the gradient of bacteria on DCGs with a greater ice velocity is a unique geographic pattern due to the increasing thickness of debris near the glacier terminus. This could also be why both bacteria and fungi showed no such gradient pattern on DGB - because DGB has a lower acclivity and shows no variation in debris thickness with distance from the glacier terminus.

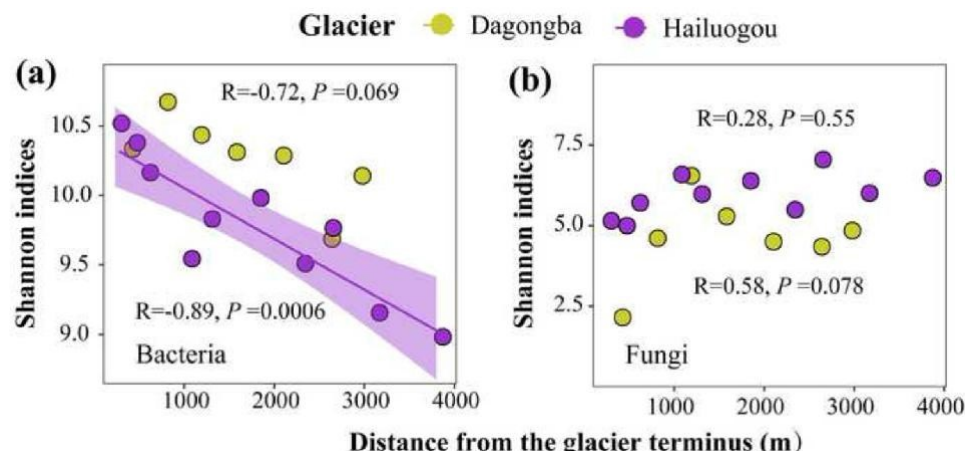


**Fig. 5.** Relationship between distance from the glacier terminus and microbial Shannon diversity of the debris-covered Dagongba and Hailuogou Glaciers, Sichuan, China. Pearson's correlation with 95% confidence interval, and at significant level of  $p < 0.05$ .

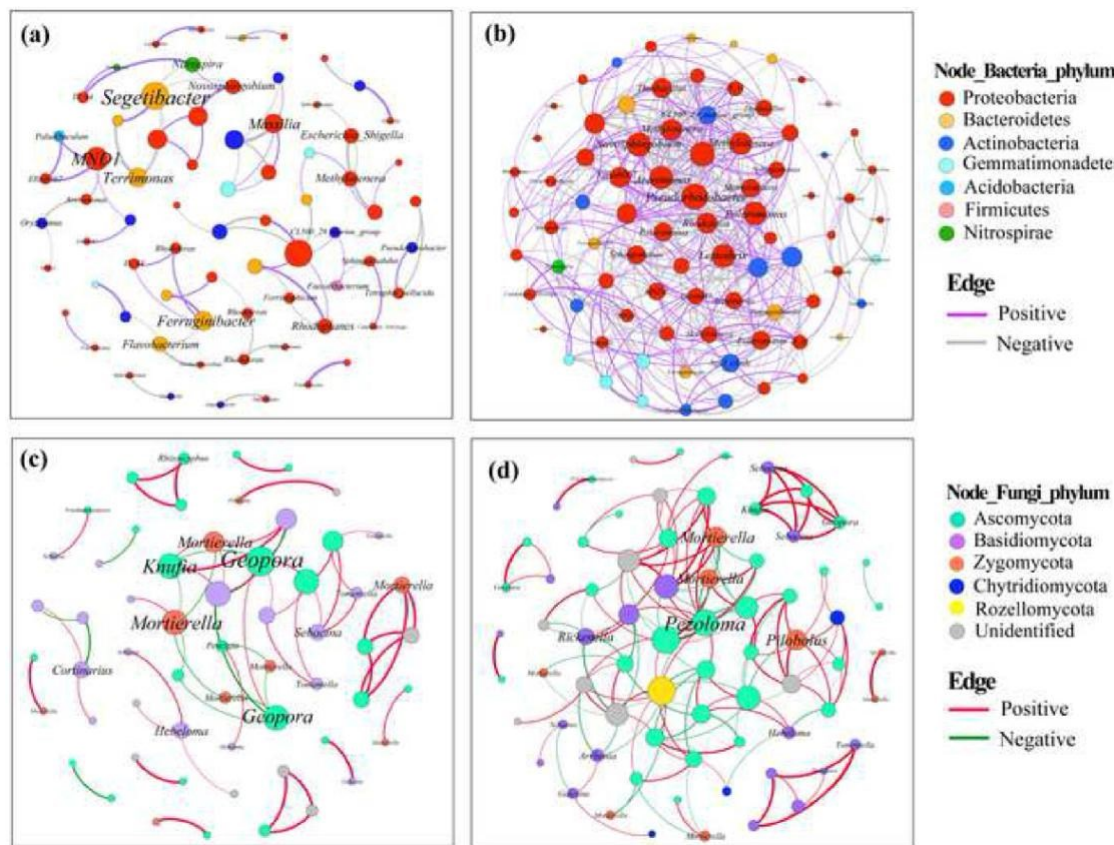


**Fig. 6.** Bacterial (a & b) and fungal (c & d) co-occurrence networks of Dangongba (left) and Hailuogou (right) Glaciers. Edges in the network indicate strong and significant ( $|r| > 0.6$ ,  $p < 0.01$ ) Spearman's correlations, color of edges indicate positive or negative correlations, the thickness of the edges indicate the intensity ( $|R|$ ) of correlations. Each node in the network represents one individual OTU. Phylum names are indicated by different colors, genus names are in italics, and the sizes of the nodes reflect their degree of connection (edge numbers assigned to the node).

#### 4.2. Microbial co-occurrence pattern and keystone taxa on supraglacial debris

Co-occurrence network analyses have been well-documented in soil ecosystems (Barberan et al., 2012; Burns and Strauss, 2011). But in glacier ecosystems, co-occurrence network analysis has only been used to explore co-existing microbial species and microbial assembly processes in glacier forefield soils (Jiang et al., 2019) and proglacial streams (Hu et al., 2020; Ren and Gao, 2019). In high-Arctic glacier forefields, it was reported that microbial co-occurrence networks tend to be more connected in habitats that are more extreme and less productive (Dong et al., 2022). Consistent with these findings, both bacterial and fungal co-occurrence were more connected and less modularized in the HLG Glacier debris. The value of modularity indices  $> 0.4$  indicates that a network has a modular structure and tends to be more stable (Newman, 2006), but high environmental stress may weaken the stability of microbial networks (Hernandez et al., 2021).

In terrestrial soils, superior climatic conditions such as high temperature and abundant precipitation generally allow for the fast formation of a stable microbial community and more diverse soil microbiomes compared with lower-temperature dry soils (Yu et al., 2023; Zhou et al., 2016). Supraglacial debris of DCGs in high-elevation cold environments represents an early developing 'extreme' habitat, which appears to be sensitive to disturbances such as fast-flowing ice and high precipitation. These conditions both exist at the HLG Glacier. Unstable ice surface conditions are found on fast-flowing ice, with shifting patches of debris as the ice melts unevenly. Greater amounts of precipitation received during the monsoonal ablation season add to available meltwater for microbial community development but may

cause a deleterious flushing effect on microbial communities. Overall, less disturbed supraglacial conditions are crucial for microbes to form stable communities on DCGs.

The bacterial co-occurrence network constructed with bacterial data for the HLG Glacier was highly connected, which means that the network could easily be dismantled by the removal (i.e., death) of the hub species. Hub taxa of the supraglacial debris from DGB and HLG Glacier include the bacteria genera *Segetibacter*, *Pseudorhodobacter*, and *Polaromonas* and the fungi genera *Geopora*, *Pezoloma*, and *Mortierella* from the co-occurrence network. These hub species play a key role in structuring microbial co-occurrence networks of the supraglacial debris on these two monsoonal temperate glaciers. The Proteobacteria *Polaromonas* and *Pseudorhodobacter* may be crucial for the assemblage of microbial communities in cold and harsh environments because they have been isolated from cold environments around the world (Zhang et al., 2010; Zhang et al., 2015; Zhang et al., 2016b). Specifically, the genus *Polaromonas*, which has a highly successful dispersal capacity, can capture organic carbon energy directly from the atmosphere via carbon monoxide dehydrogenase genes (Ambrosini et al., 2017; Gawor et al., 2016). Moreover, *Polaromonas* can degrade labile compounds (Coenye, 2013), making them one of the earliest-colonizing bacteria in newly exposed habitats (Hanson et al., 2012). *Polaromonas* has also been reported to be dominant in glacial habitats worldwide including on glacial ice, sediments, debris, and cryoconite holes (Ambrosini et al., 2017; Franzetti et al., 2013; Gawor et al., 2016). The ectomycorrhizal fungi *Geopora* was the hub taxa in the co-occurrence network of DGB and was documented in one study to be diverse in nutrient-limited glacial fore-field (Botnen et al., 2020). Some species within *Pezoloma* are the mycorrhizal fungi of plants (Becquer et al., 2018; Kowal et al., 2016);

Peintner et al., 2001). *Mortierella* is a genus of filamentous fungi within the Zygomycetes and has been found in the glacial forefield (Telagathoti et al., 2021). From our findings, it is suggested to explore other debris-covered glacier surfaces to examine if these hub species may be considered keystone species in worldwide glacier debris microbial communities.

## 5. Conclusion

Collectively, we found that supraglacial debris harbors diverse bacterial and fungal communities which represent a significant and unique microbial hotspot. Debris-covered glaciers with different microclimates, geology, and surface conditions, harbor unique microbial communities and show great variations in microbial diversity and co-occurrence networks, even though they are geographically adjacent. A chronosequence exists on the surface of typical DCGs similar to chronosequences reported from glacier forefields, while debris near the glacier terminus had a longer exposure period which creates a more stable environment, which is more suitable for the colonization and development of diverse bacterial communities. A more stable and old supraglacial debris controlled by the thicker debris and low surface velocity shapes the less-connected but more modularized co-occurrence networks of both bacterial and fungal communities. This study provides key insights into mechanisms that drive the establishment and early assembly of microbial communities in debris-covered glacier environments.

## Funding

This research has been supported by the Sichuan Science and Technology Program (grant no. 2020JDJQ0002 and 2021JDJQ0009), the National Natural Science Foundation of China (grant no. 41877338), and the National Science Foundation (NSF) Postdoctoral Research Fellowships in Biology (grant no. 2010852).

## Declaration of Competing Interest

The authors declare that they have no known competing financial interests or personal relationships that could have appeared to influence the work reported in this paper.

## Data Availability

Sequencing data for bacterial and fungal communities were deposited in the National Center for Biotechnology Information (NCBI) Sequence Read Archive (<http://trace.ncbi.nlm.nih.gov/Traces/sra/>) under the accession numbers of PRJNA797905 (bacteria) and PRJNA798561 (fungi).

## Acknowledgments

We thank anonymous reviewers for their suggestions in writing and analysis. We thank the Mt. Gongga Alpine Ecosystem Observation and Research Station, Chinese Academy of Sciences, for environmental data collection and field assistance. Special thanks also go to Hongmao Jiang, Haijun Liao, and Yan Zhong for the assistance in data analysis and debris samples collection.

## Author's contribution

X.L. and Q.L. conceived and supervised the project. Y.H. and H.F. analyzed data and wrote the manuscript. Q.L. and Y.H. collected samples in field, Z.W. and B.D. assisted in data analysis and conceived the ideas. All authors have contributed substantially to the revisions.

## Appendix A. Supporting information

Supplementary data associated with this article can be found in the online version at doi:10.1016/j.micres.2023.127409.

## References

Altschul, S.F., Gish, W., Miller, W., Myers, E.W., Lipman, D.J., 1990. Basic local alignment search tool. *J. Mol. Biol.* 215 (3), 403–410. [https://doi.org/10.1016/s0022-2836\(05\)80360-2](https://doi.org/10.1016/s0022-2836(05)80360-2).

Ambrosini, R., Musitelli, F., Navarra, F., Tagliaferri, I., Gandolfi, I., Bestetti, G., Mayer, C., Minora, U., Azzoni, R.S., Diolaiuti, G., Smiraglia, C., Franzetti, A., 2017. Diversity and assembling processes of bacterial communities in cryoconite holes of a Karakoram Glacier. *Microb. Ecol.* 73 (4), 827–837. <https://doi.org/10.1007/s00248-016-0914-6>.

Azzoni, R.S., Franzetti, A., Fontaneto, D., Zullini, A., Ambrosini, R., 2015. Nematodes and rotifers on two Alpine debris-covered glaciers. *Ital. J. Zool.* 82, 616–623. <https://doi.org/10.1080/11250003.2015.1080312>.

Banerjee, S., Schlaeppi, K., van der Heijden, M.G.A., 2018. Keystone taxa as drivers of microbiome structure and functioning. *Nat. Rev. Microbiol.* 16, 567–576. <https://doi.org/10.1038/s41579-018-0024-1>.

Bao, S., 2000. *Soil and Agricultural Chemistry Analysis*. China Agriculture Press, Beijing. (in chinese).

Barberan, A., Bates, S.T., Casamayor, E.O., Fierer, N., 2012. Using network analysis to explore co-occurrence patterns in soil microbial communities. *ISME J.* 6, 343–351. <https://doi.org/10.1038/ismej.2011.119>.

Bastian, M., Heymann, S., Jacomy, M., 2009. Gephi: an open source software for exploring and manipulating networks. *Third Int. ICWSM Conf.* 361–362. <https://www.aai.org/ocs/index.php/ICWSM/09/paper/view/154>.

Becquer, A., Garcia, K., Amenc, L., Rivard, C., Dore, J., Trives-Segura, C., Szponarski, W., Russel, S., Baeza, Y., Lassalle-Kaiser, B., Gay, G., Zimmermann, S.D., Plassard, C., 2018. The *Hebeloma cylindrosporum* HcPT2 Pi transporter plays a key role in ectomycorrhizal symbiosis. *N. Phytol.* 220 (4), 1185–1199. <https://doi.org/10.1111/nph.15281>.

Benjamini, Y., Hochberg, Y., 1995. Controlling the false discovery rate - a practical and powerful approach to Multiple Testing. *J. R. Stat. Soc., Ser. B* 57, 289–300. <https://doi.org/10.2307/2346101>.

Bolger, A.M., Lohse, M., Usadel, B., 2014. Trimmomatic: a flexible trimmer for Illumina sequence data. *Bioinformatics* 30 (15), 2114–2120. <https://doi.org/10.1093/bioinformatics/btu170>.

Botnen, S.S., Mundra, S., Kauserud, H., Eidesen, P.B., 2020. Glacier retreat in the High Arctic: opportunity or threat for ectomycorrhizal diversity? *FEMS Microbiol. Ecol.* 96 (12) <https://doi.org/10.1093/femsec/fiaa171>.

Brown, S.P., Jumpponen, A., 2014. Contrasting primary successional trajectories of fungi and bacteria in retreating glacier soils. *Mol. Ecol.* 23 (2), 481–497. <https://doi.org/10.1111/mec.12487>.

Burns, J.H., Strauss, S.Y., 2011. More closely related species are more ecologically similar in an experimental test. *PNAS* 108 (13), 5302–5307. <https://doi.org/10.1073/pnas.1013003108>.

Caccianiga, M., Andreis, C., Diolaiuti, G., D'Agata, C., Mihalcea, C., Smiraglia, C., 2011. Alpine debris-covered glaciers as a habitat for plant life. *Holocene* 21, 1011–1020. <https://doi.org/10.1177/0959683611400219>.

Caporaso, J.G., Kuczynski, J., Stombaum, J., Bittinger, K., Bushman, F.D., Costello, E.K., Fierer, N., Pena, A.G., Goodrich, J.K., Gordon, J.I., Huttley, G.A., Kelley, S.T., Knights, D., Koenig, J.E., Ley, R.E., Lozupone, C.A., McDonald, D., Muegge, B.D., Pirrung, M., Reeder, J., Sevinsky, J.R., Turnbaugh, P.J., Walters, W.A., Widmann, J., Yatsunenko, T., Zaneveld, J., Knight, R., 2010. QIIME allows analysis of high-throughput community sequencing data. *Nat. Methods* 7 (5), 335–336. <https://doi.org/10.1038/nmeth.1303>.

Coenye, T., 2013. The Family Burkholderiaceae. The Prokaryotes: Alphaproteobacteria and Betaproteobacteria. Springer, Berlin, Heidelberg, pp. 759–776. [https://doi.org/10.1007/978-3-642-30197-1\\_239](https://doi.org/10.1007/978-3-642-30197-1_239).

Compagno, L., Huss, M., Miles, E., McCarthy, M., Zekollari, H., Pellicciotti, F., Farinotti, D., 2022. Modelling supraglacial debris-cover evolution from the single glacier to the regional scale: an application to High Mountain Asia. *Cryosphere* 16, 1697–1718. <https://doi.org/10.5194/tc-16-1697-2022>.

Darcy, J.L., Schmidt, S.K., 2016. Nutrient limitation of microbial phototrophs on a debris-covered glacier. *Soil Biol. Biochem.* 95, 156–163. <https://doi.org/10.1016/j.soilbio.2015.12.019>.

Darcy, J.L., King, A.J., Gendron, E.M.S., Schmidt, S.K., 2017. Spatial autocorrelation of microbial communities atop a debris-covered glacier is evidence of a supraglacial chronosequence. *FEMS Microbiol. Ecol.* 93 (8) <https://doi.org/10.1093/femsec/fix095>.

Dixon, P., 2003. VEGAN, a package of R functions for community ecology. *J. Veg. Sci.* 14 (6), 927–930. <https://doi.org/10.1111/j.1654-1103.2003.tb02228.x>.

Dong, K., Yu, Z., Kerfah, D., Lee, S.S., Li, N., Yang, T., Adams, J.M., 2022. Soil microbial co-occurrence networks become less connected with soil development in a high Arctic glacier foreland succession. *Sci. Total Environ.* 813, 152565. <https://doi.org/10.1016/j.scitotenv.2021.152565>.

Dzurendova, S., Zimmermann, B., Kohler, A., Reitzel, K., Nielsen, U.G., Dupuy-Galet, B. X., Leivers, S., Horn, S.J., Shapaval, V., 2021. Calcium affects polyphosphate and lipid accumulation in mucoromycota fungi. *J. Fungi* 7 (4), 300. <https://doi.org/10.3390/jof7040300>.

Fernandez-Martinez, M.A., Perez-Ortega, S., Pointing, S.B., Allan Green, T.G., Pintado, A., Rozzi, R., Sancho, L.G., de los Rios, A., 2017. Microbial succession dynamics along glacier forefield chronosequences in Tierra del Fuego (Chile). *Polar Biol.* 40 (10), 1939–1957. <https://doi.org/10.1007/s00300-017-2110-7>.

Fickert, T., Friend, D., Molnia, B., Grueninger, F., Richter, M., 2022. Vegetation ecology of debris-covered glaciers (DCGs)-site conditions, vegetation patterns and implications for DCGs serving as quaternary cold- and warm-stage plant refugia. *Diversity* 14 (2) <https://doi.org/10.13399/d14020114>.

Franzetti, A., Tatangelo, V., Gandolfi, I., Bertolini, V., Bestetti, G., Diolaiuti, G., D'Agata, C., Mihalcea, C., Smiraglia, C., Ambrosini, R., 2013. Bacterial community structure on two alpine debris-covered glaciers and biogeography of Polaromonas phylotypes. *ISME J.* 7 (8), 1483–1492. <https://doi.org/10.1038/ismej.2013.48>.

Franzetti, A., Pittino, F., Gandolfi, I., Azzone, R.S., Diolaiuti, G., Smiraglia, C., Pelfini, M., Compostella, C., Turchetti, B., Buzzini, P., Ambrosini, R., 2020. Early ecological succession patterns of bacterial, fungal and plant communities along a chronosequence in a recently deglaciated area of the Italian Alps. *FEMS Microbiol. Ecol.* 96 (10) <https://doi.org/10.1093/femsec/fiaa165>.

Fu, Y., Liu, Q., Liu, G., Zhang, B., Zhang, R., Cai, J., Wang, X., Xiang, W., 2021. Seasonal ice dynamics in the lower ablation zone of Dagongba Glacier, southeastern Tibetan Plateau, from multitemporal UAV images. *J. Glaciol.* 68, 1–15. <https://doi.org/10.1017/jog.2021.123>.

Gao, C.H., Yu, G., Cai, P., 2021. ggVennDiagram: an intuitive, easy-to-use, and highly customizable R package to generate venn diagram. *Front. Genet* 12, 1598. <https://doi.org/10.3389/fgene.2021.706907>.

Gawor, J., Grzesiak, J., Sasin-Kurowska, J., Borsuk, P., Gromadka, R., Gorniak, D., Swiatecki, A., Aleksandrzak-Piekarczyk, T., Zdanowski, M.K., 2016. Evidence of adaptation, niche separation and microevolution within the genus Polaromonas on Arctic and Antarctic glacial surfaces. *Extremophiles* 20 (4), 403–413. <https://doi.org/10.1007/s00792-016-0831-0>.

Gobbi, M., Isaia, M., De Bernardi, F., 2011. Arthropod colonisation of a debris-covered glacier. *Holocene* 21. <https://doi.org/10.1177/0959683610374885>.

Hanson, B., Yagi, J., Jeon, C., Madsen, E., 2012. Role of nitrogen fixation in the autecology of Polaromonas naphthalenivorans in contaminated sediments. *Environ. Microbiol.* 14, 1544–1557. <https://doi.org/10.1111/j.1462-2920.2012.02743.x>.

Hernandez, D.J., David, A.S., Menges, E.S., Searcy, C.A., Afkhami, M.E., 2021. Environmental stress destabilizes microbial networks. *ISME J.* 15 (6), 1722–1734. <https://doi.org/10.1038/s41396-020-00882-x>.

Herreid, S., Pellicciotti, F., 2020. The state of rock debris covering Earth's glaciers. *Nat. Geo* 13 (9), 621–627. <https://doi.org/10.1038/s41561-020-0615-0>.

Hu, Y., Yao, X., Wu, Y., Han, W., Zhou, Y., Tang, X., Shao, K., Gao, G., 2020. Contrasting patterns of the bacterial communities in melting ponds and periglacial Rivers of the Zhuxi glacier in the Tibet Plateau. *Microorganisms* 8 (4). <https://doi.org/10.3390/microorganisms8040509>.

Jiang, Y., Lei, Y., Yang, Y., Korpelainen, H., Niinemets, Ü., Li, C., 2018. Divergent assemblage patterns and driving forces for bacterial and fungal communities along a glacier forefield chronosequence. *Soil Biol. Biochem.* 118, 207–216. <https://doi.org/10.1016/j.soilbio.2017.12.019>.

Jiang, Y.L., Song, H.F., Lei, Y.B., Korpelainen, H., Li, C.Y., 2019. Distinct co-occurrence patterns and driving forces of rare and abundant bacterial subcommunities following a glacial retreat in the eastern Tibetan Plateau. *Biol. Fertil. Soils* 55 (4), 351–364. <https://doi.org/10.1007/s00374-019-01355-w>.

Kersters, K., De Vos, P., Gillis, M., Swings, J., Vandamme, P., Stackebrandt, E., 2006. Introduction to the Proteobacteria. In: Dworkin, M., Falkow, S., Rosenberg, E., Schleifer, K.-H., Stackebrandt, E. (Eds.), *The Prokaryotes: Volume 5: Proteobacteria: Alpha and Beta Subclasses*. Springer New York, New York, NY, pp. 3–37.

Kowal, J., Pressel, S., Duckett, J.G., Bidartondo, M.I., 2016. Liverworts to the rescue: an investigation of their efficacy as mycorrhizal inoculum for vascular plants. *Funct. Ecol.* 30 (6), 1014–1023. <https://doi.org/10.1111/1365-2435.12580>.

Langfelder, P., Horvath, S., 2008. WGCNA: an R package for weighted correlation network analysis. *BMC Bioinforma.* 9, 559. <https://doi.org/10.1186/1471-2105-9-559>.

Li, Z., He, Y., Yang, X., Theakstone, W.H., Jia, W., Pu, T., Liu, Q., He, X., Song, B., Zhang, N., Wang, S., Du, J., 2010. Changes of the Hailuogou glacier, Mt. Gongga, China, against the background of climate change during the Holocene. *Quat. Int* 218 (1), 166–175. <https://doi.org/10.1016/j.quaint.2008.09.005>.

Liao, H., Liu, Q., Zhong, Y., Lu, X., 2020. Supraglacial debris-cover change and its spatial heterogeneity in the Mount Gongga, 1990–2019. *Acta Geogr. Sin.* 76, 2647–2659 (In Chinese).

Liao, H., Liu, Q., Zhong, Y., Lu, X., 2020. Landsat-based estimation of the glacier surface temperature of Hailuogou Glacier, Southeastern Tibetan Plateau, Between 1990 and 2018. *Remote Sens.* 12 (13) <https://doi.org/12.10.3390/rs12132105>.

Liu, G., Zhang, H., Fu, Y., Chen, Y.X., Shi, L., 2009. Sedimentary characteristics and subglacial processes of the glacial deposits in Hailuogou Glacier, Gongga Mountain. *J. Glaciol.* 51, 68–74 (In Chinese).

Liu, Q., Liu, S., 2015a. Response of glacier mass balance to climate change in the Tianshan Mountains during the second half of the twentieth century. *Clim. Dyn.* 46 (1–2), 303–316. <https://doi.org/10.1007/s00382-015-2585-2>.

Liu, Q., Liu, S., Zhang, Y., Wang, X., Zhang, Y., Guo, W., Xu, J., 2017. Recent shrinkage and hydrological response of Hailuogou Glacier, a monsoon temperate glacier on the east slope of Mount Gongga, China. *J. Glaciol.* 56, 215–224. <https://doi.org/10.3189/002214310791968520>.

Liu, S., Hou, Y.L., Liu, W., Lu, C., Wang, W., Sun, S., 2015b. Components of the calcium-calcineurin signaling pathway in fungal cells and their potential as antifungal targets. *Eukaryot. Cell* <https://doi.org/10.1128/EC.00271-14>.

Liu, Y., Ji, M., Yu, T., Zaugg, J., Anesio, A.M., Zhang, Z., Hu, S., Hugenholtz, P., Liu, K., Liu, P., Chen, Y., Luo, Y., Yao, T., 2022. A genome and gene catalog of glacier microbiomes. *Nat. Biotechnol.* 40, 1341–1348. <https://doi.org/10.1038/s41587-022-01367-2>.

Ma, L., Li, B., Jiang, X.T., Wang, Y.L., Xia, Y., Li, A.D., Zhang, T., 2017. Catalogue of antibiotic resistome and host-tracking in drinking water deciphered by a large scale survey. *Microbiome* 5 (1), 154. <https://doi.org/10.1186/s40168-017-0369-0>.

Mendiburu, F., 2010. *Agricolae: statistical procedures for agricultural research. R. Package Version 1, 1–8*.

de Menezes, A.B., Richardson, A.E., Thrall, P.H., 2017. Linking fungal–bacterial co-occurrences to soil ecosystem function. *Curr. Opin. Microbiol.* 37, 135–141. <https://doi.org/10.1016/j.mib.2017.06.006>.

Miles, K.E., Hubbard, B., Irvine-Fynn, T.D.L., Miles, E.S., Quincey, D.J., Rowan, A.V., 2020. Hydrology of debris-covered glaciers in High Mountain Asia. *Earth-Sci. Rev.* 207, 103212. <https://doi.org/10.1016/j.earscirev.2020.103212>.

Mukherjee, P.K., Chandra, J., Retuerto, M., Sikaroodi, M., Brown, R.E., Jurevic, R., Salata, R.A., Lederman, M.M., Gillevet, P.M., Ghamoum, M.A., 2014. Oral mycobiome analysis of HIV-infected patients: identification of *Pichia* as an antagonist of opportunistic fungi. *e1003996-e1003996 PLoS Pathog.* 10 (3). <https://doi.org/10.1371/journal.ppat.1003996>.

Newman, M.E., 2006. Modularity and community structure in networks. *PNAS* 103 (23), 8577–8582. <https://doi.org/10.1073/pnas.0601602103>.

Nossa, C.W., Oberdorf, W.E., Yang, L., Aas, J.A., Paster, B.J., Desantis, T.Z., Brodie, E.L., Malamud, D., Poles, M.A., Pei, Z., 2010. Design of 16S rRNA gene primers for 454 pyrosequencing of the human foregut microbiome. *World J. Gastroenterol.* 16 (33), 4135–4144. <https://doi.org/10.3748/wjg.v16.i33.4135>.

Peintner, U., Bouger, N., Castellano, M., Moncalvo, J.M., Moser, M., Trappe, J., Vilgalys, R., 2001. Multiple origins of sequestrate fungi related to *Cortinarius* (Cortinariaceae). *Am. J. Bot.* 88, 2168–2179. <https://doi.org/10.2307/3558378>.

Perini, L., Gostinčar, C., Gunde-Cimerman, N., 2019a. Fungal and bacterial diversity of Svalbard subglacial ice. *Sci. Rep.* 9, 20230. <https://doi.org/10.1038/s41598-019-56290-5>.

Perini, L., Gostinčar, C., Anesio, A.M., Williamson, C., Tranter, M., Gunde-Cimerman, N., 2019b. Darkening of the Greenland Ice Sheet: Fungal abundance and diversity are associated with algal bloom, 557–557 *Front. Microbiol.* 10. <https://doi.org/10.3389/fmicb.2019.00557>.

RCoreTeam. R: A language and environment for statistical computing R Foundation for Statistical Computing, Vienna, Austria 2021.

Ren, Z., Gao, H., 2019. Ecological networks reveal contrasting patterns of bacterial and fungal communities in glacier-fed streams in Central Asia. *Peer J.* 7. <https://doi.org/10.7717/peerj.7715>.

Reyon, D., Tsai, S.Q., Khayter, C., Foden, J.A., Sander, J.D., Joung, J.K., 2012. FLASH assembly of TALENs for high-throughput genome editing. *Nat. Biotechnol.* 30 (5), 460–465. <https://doi.org/10.7717/peerj.7715>.

Rognes, T., Flouri, T., Nichols, B., Quince, C., Mahé, F., 2016. VSEARCH: a versatile open source tool for metagenomics. *PeerJ*. <https://doi.org/10.7717/peerj.2584>.

Sajjad, W., Ali, B., Bahadur, A., Ghimire, P.S., Kang, S., 2021. Bacterial diversity and communities structural dynamics in soil and meltwater runoff at the frontier of Baishui Glacier No.1, China. *Microb. Ecol.* 81 (2), 370–384. <https://doi.org/10.1007/s00248-020-01600-y>.

Scherler, D., Wulf, H., Gorelick, N., 2018. Global assessment of supraglacial debris-cover extents, 798–711,805 *Geophys. Res. Lett.* 45 (21), 11. <https://doi.org/10.1029/2018GL080158>.

Schmidt, S.K., Porazinska, D., Concienne, B.L., Darcy, J.L., King, A.J., Nemergut, D.R., 2016. Biogeochemical stoichiometry reveals P and N limitation across the post-glacial landscape of Denali National Park, Alaska. *Ecosystems* 19 (7), 1164–1177. <https://doi.org/10.1007/s10021-016-9992-z>.

Schoch, C.L., Seifert, K.A., Huhndorf, S., Robert, V., Spouge, J.L., Levesque, C.A., Chen, W., 2012. Nuclear ribosomal internal transcribed spacer (ITS) region as a universal DNA barcode marker for Fungi. *PNAS* 109 (16), 6241–6246. <https://doi.org/10.1073/pnas.1117018109>.

Searle, M., Roberts, N., Chung, S.L., Lee, Y.H., Cook, K., Elliott, J., Weller, O., St-Onge, M., Xu, X., Tan, X., Li, K., 2016. Age and anatomy of the Gongga Shan batholith, eastern Tibetan Plateau, and its relationship to the active Xianshuihe fault. *Geosphere* 12 (3), 948–970. <https://doi.org/10.1130/GES01244.1>.

Shen, C., Gunina, A., Luo, Y., Wang, J., He, J.-Z., Kuzyakov, Y., Hemp, A., Classen, A.T., Ge, Y., 2020. Contrasting patterns and drivers of soil bacterial and fungal diversity across a mountain gradient. *Environ. Microbiol.* 22 (8), 3287–3301. <https://doi.org/10.1111/1462-2920.15090>.

Sherpa, M.T., Najar, I.N., Das, S., Thakur, N., 2018. Bacterial diversity in an alpine debris-free and debris-cover accumulation zone Glacier Ice, North Sikkim, India. *Indian J. Microbiol.* 58 (4), 470–478. <https://doi.org/10.1007/s12088-018-0747-8>.

Sherpa, M.T., Najar, I.N., Das, S., Thakur, N., 2021. Exploration of microbial diversity of himalayan glacier moraine soil using 16S amplicon sequencing and phospholipid fatty acid analysis approaches. *Curr. Opin. Microbiol.* 78 (1), 78–85. <https://doi.org/10.1007/s00284-020-02259-x>.

Smith, H.J., Dieser, M., McKnight, D.M., SanClements, M.D., Foreman, C.M., 2018. Relationship between dissolved organic matter quality and microbial community composition across polar glacial environments. *FEMS Microbiol Ecol.* 94 (7). <https://doi.org/10.1093/femsec/fiy090>.

Somerfield, P.J., Clarke, K.R., Gorley, R.N., 2021. Analysis of similarities (ANOSIM) for 3-way designs. *Austral Ecol.* 46 (6), 927–941. <https://doi.org/10.1111/aec.13083>.

Steinhauser, D., Krall, L., Müsing, C., Büssem, D., Usadel, B., 2008. Correlation networks. *Anal. Biol. Netw.* 305–333. <https://doi.org/10.1002/9780470253489.ch13>.

Su, Z., Liang, D., Hong, M., 1993. Developing conditions, amounts and distributions of glaciers in Gongga Mountains. *J. Glaciol. Geocryol.* 15, 551–558.

Su, Z., Song, G., Cao, Z., 1996. Maritime characteristics of Hailuogou glacier in the Gongga Mountains. *J. Glaciol. Geocryol.* S1: 51–59 (In Chinese).

Sun, S., Li, S., Avera, B.N., Strahm, B.D., Badgley, B.D., 2017. Soil bacterial and fungal communities show distinct recovery patterns during forest ecosystem restoration. *Appl. Environ. Microbiol.* 83 (14). <https://doi.org/10.1128/aem.00966-17>.

Telagathoti, A., Probst, M., Peintner, U., 2021. Habitat, snow-cover and soil pH, affect the distribution and diversity of mortierellaceae species and their associations to bacteria. *Front. Microbiol.* 12, 669784. <https://doi.org/10.3389/fmicb.2021.669784>.

de Vries, F.T., Griffiths, R.I., Bailey, M., Craig, H., Girlanda, M., Gweon, H.S., Hallin, S., Kaisermann, A., Keith, A.M., Kretzschmar, M., Lemanceau, P., Lumini, E., Mason, K.E., Oliver, A., Ostle, N., Prosser, J.I., Thion, C., Thomson, B., Bardgett, R.D., 2018. Soil bacterial networks are less stable under drought than fungal networks. *Nat. Commun.* 9 (1), 3033. <https://doi.org/10.1038/s41467-018-05516-7>.

Wagg, C., Schlaeppi, K., Banerjee, S., Kuramae, E.E., van der Heijden, M.G.A., 2019. Fungal-bacterial diversity and microbiome complexity predict ecosystem functioning. *Nat. Commun.* 10 (1), 4841. <https://doi.org/10.1038/s41467-019-12798-y>.

Wang, Q., Garrity, G.M., Tiedje, J.M., Cole, J.R., 2007. Naive Bayesian classifier for rapid assignment of rRNA sequences into the new bacterial taxonomy. *Appl. Environ. Microbiol.* 73 (16), 5261–5267. <https://doi.org/10.1128/aem.00062-07>.

Wei, T., & Simko, V., 2017. R package "corrplot": Visualization of a Correlation Matrix. <https://github.com/taiyun/corrplot>.

Westoby, M.J., Rounce, D.R., Shaw, T.E., Fyffe, C.L., Moore, P.L., Stewart, R.L., Brock, B.W., 2020. Geomorphological evolution of a debris-covered glacier surface. *Earth Surf. Process. Landf.* 45 (14), 3431–3448. <https://doi.org/10.1002/esp.4973>. Wickham, H., 2016. *ggplot2: Elegant Graphics for Data Analysis*. Springer-Verlag, New York.

Winter-Billington, A., Dadić, R., Moore, R.D., Flerchinger, G., Wagnon, P., Banerjee, A., 2022. Modeling debris-covered glacier ablation using the simultaneous heat and water transport model. Part 1: Model Dev. *Appl. North Chang. Nup. Front. Earth Sci.* 10. <https://doi.org/10.3389/feart.2022.796877>.

Wu, L., Wen, C., Qin, Y., Yin, H., Tu, Q., Van Nostrand, J.D., Yuan, T., Yuan, M., Deng, Y., Zhou, J., 2015. Phasing amplicon sequencing on Illumina MiSeq for robust environmental microbial community analysis. *BMC Microbiol.* 15 (1), 125. <https://doi.org/10.1186/s12866-015-0450-4>.

Wu, X., Zhang, H., Chen, J., Shang, S., Wei, Q., Yan, J., Tu, X., 2016. Comparison of the fecal microbiota of dholes high-throughput Illumina sequencing of the V3–V4 region of the 16S rRNA gene. *Appl. Microbiol. Biotechnol.* 100 (8), 3577–3586. <https://doi.org/10.1007/s00253-015-7257-y>.

Yu, H., Li, L., Ma, Q., Liu, X., Li, Y., Wang, Y., et al., 2023. Soil microbial responses to large changes in precipitation with nitrogen deposition in an arid ecosystem. *Ecology*. <https://doi.org/10.1002/ecy.4020>.

Zhang, L., Delgado-Baquerizo, M., Shi, Y., Liu, X., Yang, Y., Chu, H., 2021. Co-existing water and sediment bacteria are driven by contrasting environmental factors across glacier-fed aquatic systems. *Water Res.* 198, 117139. <https://doi.org/10.1016/j.watres.2021.117139>.

Zhang, S., Yang, G., Wang, Y., Hou, S., 2010. Abundance and community of snow bacteria from three glaciers in the Tibetan Plateau. *J. Environ. Sci.* 22 (9), 1418–1424. [https://doi.org/10.1016/S1001-0742\(09\)60269-2](https://doi.org/10.1016/S1001-0742(09)60269-2).

Zhang, S.H., Hou, S.G., Qin, X., Du, W.T., Liang, F., Li, Z.G., 2015. Preliminary study on effects of glacial retreat on the dominant glacial snow bacteria in Laohugou Glacier No. 12. *Geomicrobiol.* J 32 (2), 113–118. <https://doi.org/10.1080/01490451.2014.929761>.

Zhang, Y., Fujita, K., Liu, S., Liu, Q., Nuimura, T., 2011. Distribution of debris thickness and its effect on ice melt at Hailuogou glacier, southeastern Tibetan Plateau, using in situ surveys and ASTER imagery. *J. Glaciol.* 57 (206), 1147–1157. <https://doi.org/10.3189/002214311798843331>.

Zhang, Y., Hirabayashi, Y., Fujita, K., Liu, S., Liu, Q., 2016a. Heterogeneity in supraglacial debris thickness and its role in glacier mass changes of the Mount Gongga. *Sci. China Earth Sci.* 59 (1), 170–184. <https://doi.org/10.1007/s11430-015-5118-2>.

Zhang, Y., Jiang, F., Chang, X., Qiu, X., Ren, L., Qu, Z., Deng, S., Da, X., Kan, W., Kim, M., Fang, C., Peng, F., 2016b. *Pseudorhodobacter collinsensis* sp. nov., isolated from a till sample of an icecap front. *Int. J. Syst. Evol. Microbiol.* 66 (1), 178–183. <https://doi.org/10.1099/ijsem.0.000693>.

Zhang, Y., Liu, S., Liu, Q., Wang, X., Jiang, Z., Junfeng, W., 2019. The role of debris cover in catchment runoff: a case study of the Hailuogou catchment, South-Eastern Tibetan Plateau. *Water*. <https://doi.org/10.3390/w11122601>.

Zhao, D., Shen, F., Zeng, J., Huang, R., Yu, Z., Wu, Q.L., 2016. Network analysis reveals seasonal pattern of co-occurrence correlations between Cyanobacteria and other bacterioplankton. *Sci. Total Environ.* 573, 817–825. <https://doi.org/10.1016/j.scitotenv.2016.08.150>.

Zhou, J., Deng, Y., Shen, L., Wen, C., Yan, Q., Ning, D., Qin, Y., Xue, K., Wu, L., He, Z., Voordeckers, J.W., Nostrand, J.D.V., Buzzard, V., Michaletz, S.T., Enquist, B.J., Weiser, M.D., Kaspari, M., Waide, R., Yang, Y., Brown, J.H., 2016. Temperature mediates continental-scale diversity of microbes in forest soils. *Nat. Commun.* 7 (1), 12083. <https://doi.org/10.1038/ncomms12083>.

Zumsteg, A., Luster, J., Goransson, H., Smittenberg, R.H., Brunner, I., Bernasconi, S.M., Zeyer, J., Frey, B., 2012. Bacterial, archaeal and fungal succession in the forefield of a receding glacier. *Microb. Ecol.* 63 (3), 552–564. <https://doi.org/10.1007/s00248-011-9991-8>.